

Trajectory Perturbations of Fin-Stabilized Projectiles Due to Muzzle Blast

E. M. Schmidt,* K. S. Fansler,† and D. D. Shear‡

U. S. Army Ballistic Research Laboratory, Aberdeen Proving Ground, Md.

The flow at the muzzle of a gun during launch of fin-stabilized projectiles is investigated both experimentally and analytically. Optical and flash radio graph surveys are used to define the muzzle blast growth and projectile dynamics. Based upon the experimental results, an analysis is developed of the loadings exerted by propellant gases upon the projectile. It is shown that both in-bore and muzzle blast flowfields must be considered. The in-bore flow is modeled as a one-dimensional, unsteady expansion, whereas the muzzle blast flow is approximated as a two-dimensional, quasisteady, underexpanded jet. The effect of launch gasdynamic loadings upon projectile motion is calculated and is shown to compare favorably with experiment.

Nomenclature

A	= area of a single fin
C_L, C_M	= lift and moment coefficients
c	= speed of sound
D	= gun tube diameter
d	= distance between obturator and fins
I_y	= projectile transverse moment of inertia
L	= lift
l	= diameter of projectile
M	= Mach number
M_r^*	= relative Mach number referenced to sonic conditions
m_p	= projectile mass
n	= number of fins
P	= momentum function
V_p	= projectile launch velocity
V_r	= relative velocity between projectile and flow
X	= axial distance from muzzle
α, α'	= angle of attack and rate of change of angle of attack, mils/caliber
Δ	= distance between projectile c.g. and fins
θ	= angular deviation from intended line of fire
σ_y, σ_z	= horizontal and vertical dispersion
$()^*$	= sonic conditions
$()_i$	= conditions in gun tube prior to shot ejection

Introduction

MODERN tactics place increasing reliance upon accuracy to achieve improved first-round hit capability. Fin-stabilized projectiles are employed extensively in anti-armor, mortar, and long-range artillery applications; thus, it is of interest to examine the relative magnitude of mechanical and gasdynamic loadings which adversely affect their launch and flight. This paper presents the results of investigations of the flowfield at the muzzle of guns during launch of fin-stabilized projectiles.

When the seal between the projectile and gun tube is broken at shot ejection, the high-pressure propellant gases are released to expand freely (Fig. 1a). For subsonic propellant gas Mach numbers, $M_1 = V_p/c_1$, expansion waves propagate into the gun tube gases and create a sonic or choked condition

at the muzzle. The obturator band, or gas seal, of conventional fin-stabilized rounds is located forward on the projectile, permitting the in-bore expansion to commence prior to ejection of the fins. Passage of the expansion over the projectile generates a relative flow velocity and, possibly, transverse loadings. Once free of the gun tube, the projectile must transit the muzzle blast flowfield prior to entry into free flight. For completeness, both the in-bore and muzzle blast environment must be investigated to determine the influence of launch gasdynamics upon the projectile trajectory; however, although a number of muzzle blast analyses have been attempted, no calculations of in-bore loadings are currently available.

Oswatitsch¹ uses the method of characteristics to compute the muzzle blast flowfield development under the assumption of spherical symmetry. He demonstrates that between the muzzle and inward facing shock (Mach disk) the flow properties are independent of the highly unsteady boundary phenomena and vary only in response to the relatively slow changes in muzzle exit conditions. Based upon this result, Oswatitsch proposes a quasisteady model of the muzzle jet. Experimental results of Schmidt and Shear² support this model through observations of the geometric invariance of the propellant jet shock structure once established behind the advancing shock layer. Erdos and Del Guidice³ also assume a quasisteady jet core to compute the development of the muzzle flow along the axis of symmetry by a finite-difference technique. Their results agree well with experimental data.²

Gretler⁴ applies the Ostwatsch model in the calculation of muzzle blast loadings on a fin-stabilized projectile. He assumes that the most significant transverse forces are generated on fin surfaces during passage through the quasisteady, supersonic core of the propellant gas jet. This approach is both supported by the experimental results presented in the current paper and used as a basis for the subsequent analytical treatment. However, Gretler's work is extended by adopting a more realistic, axially symmetric flow model and by including the effects of in-bore flow. Gasdynamic loadings on the projectile in transit of the muzzle region are computed, and the relative magnitude of in-bore and muzzle blast perturbations are compared as a function of propellant gas Mach number prior to shot ejection. To verify the model experimentally, a muzzle adaptor is designed and tested which modifies the flow over the projectile. The resultant measurements of changes in the projectile trajectory due to the presence of the muzzle adaptor are compared with predictions of the present analysis.

Muzzle Blast Flow Survey

Tests⁵ were conducted using a 5.8-mm smoothbore gun firing a fin-stabilized flechette at a velocity of 1473 m/sec.

Presented at the AIAA 3rd Atmospheric Flight Mechanics Conference, Arlington, Texas, June 7-9, 1976 (in bound volume of Conference papers, no paper number); submitted Sept. 27, 1976; revision received Dec. 13, 1976.

Index categories: LV/M Trajectories and Tracking Systems; Shock Waves and Detonations.

*Aerospace Engineer. Member AIAA.

†Physicist. Member AIAA.

‡Physical Science Technician.

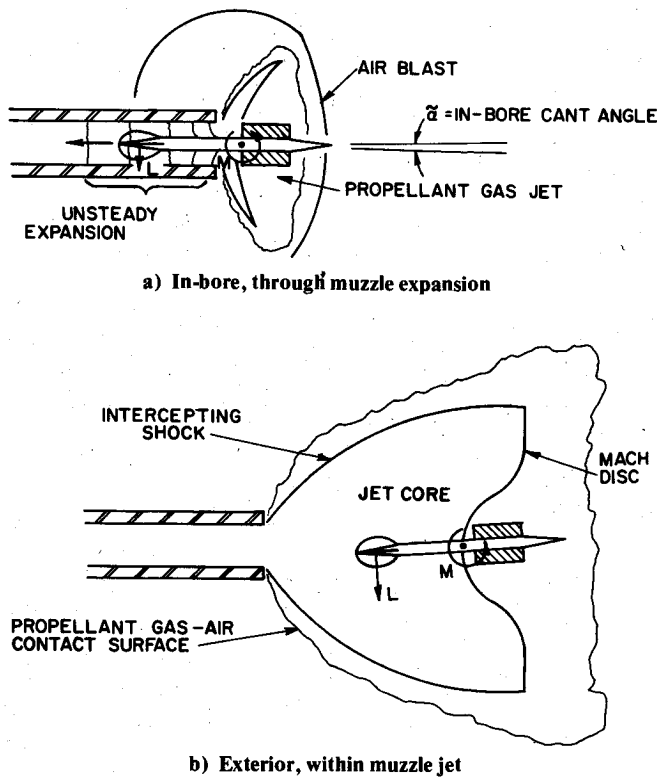


Fig. 1 Sources of gasdynamic loadings during launch.

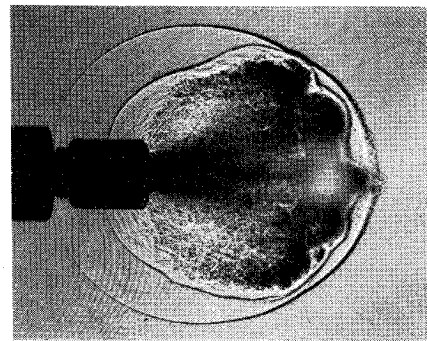
Sequential spark shadowgraphs² were taken of the developing flowfield (Fig. 2a) and orthogonal flash x-rays were used to determine the initial attitude and dynamics of the projectile (Figs. 2b and c). The spark shadowgraphs clearly show that while the forward portion of the projectile and sabot are in the unsteady shock layer, the projectile fins are immersed in the quasisteady core of the muzzle jet. From the full set of spark shadowgraph data, the motion of the Mach disk, propellant gas/air contact surface, and free air blast along the axis of symmetry may be obtained (Fig. 3).

Since the obturator is located forward on the projectile, the propellant gas is released while the fins are still in-bore. For subsonic propellant gas velocities, one-dimensional expansion waves propagate upstream (into the gun tube), accelerating the flow to a sonic velocity at the muzzle. Prior to shot ejection, the projectile and propellant gas velocities are equal; thus, passage of the expansion waves results in propellant gas flow relative to the projectile directed rear to front. External to the muzzle, the underexpanded propellant gas jet and coupled free air blast develop. The region between the muzzle and inward facing shocks forms the quasisteady supersonic core of the jet. Since the Mach disk precedes the obturator, the fins are exposed directly to this core flow. As the fins traverse this region, they experience flow from the rear which increases in Mach number (relative to the projectile) from subsonic through to low hypersonic values. Radial expansion and ambient back pressure slow the outward propagation of the blast field permitting the projectile to penetrate the shock layer.

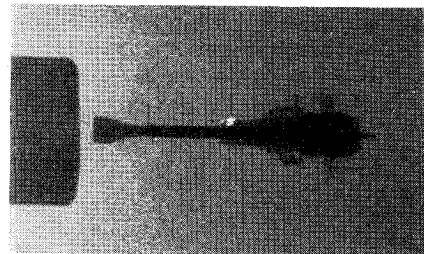
Loading Analysis

Transverse gasdynamic loadings upon the projectile will be assumed to originate solely at the fins. This approximation is substantiated by Glauz,⁶ who demonstrates that more than 95% of the transverse force generated on a slender, fin-stabilized projectile in crossflow occurs on fin surfaces. The lift on a fin may be expressed as

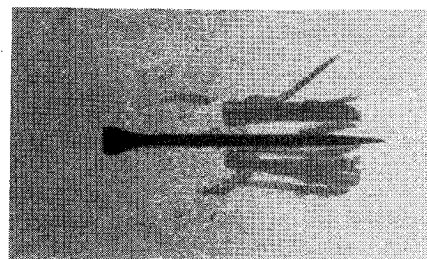
$$L = \frac{1}{2} \rho V_r^2 A C_L \quad (1)$$



a) Spark shadowgraph



b) Flash x-ray, $x/D = 0.4$



c) Flash x-ray, $X/D = 50.0$

Fig. 2 Sample of experimental data.

Following Gretler, the lift coefficient is evaluated using two-dimensional thin airfoil theory (Fig. 4). The effects of flow inclination, wingtips, and wing-body interference are neglected. These simplifications should produce an overestimation of the fin lift; thus, the predicted muzzle blast impulse is an upper bound to the actual value.

A nondimensional lift is defined as

$$\bar{L} = L / [(p^* + \rho^* c^{*2}) A \alpha] = [\gamma / 2 (\gamma + 1)] C_{L_\alpha} (\rho / \rho^*) M_r^{*2} \quad (2)$$

The value of \bar{L} is independent of fin geometry or attitude; however, it is a function of the local flow properties which vary both in space and time. Although it is possible to account for temporal variations using the quasisteady approximation,¹ it will be assumed that the propellant gases flowing into the muzzle region have constant properties during the period of shot ejection. This approximation is supported experimentally by measurements of muzzle pressure⁷ which are nearly invariant during projectile transit of the muzzle flow region. Additionally, since propellant gas properties decay during this period, this assumption is consistent with the goal of producing an upper bound to the muzzle gas impulse.

The fins must traverse two flowfields, the in-bore expansion (Fig. 1a) and the muzzle blast (Fig. 1b). The flow within the gun tube is assumed to be a one-dimensional centered expansion wave. The solution to this "similarity" flow⁸ is well known and, for flows which expand to sonic (choked) exit conditions, is only a function of the propellant gas Mach number prior to shot ejection, $M_1 = V_p / c_1$. The flow exterior to the muzzle is a complex region consisting of

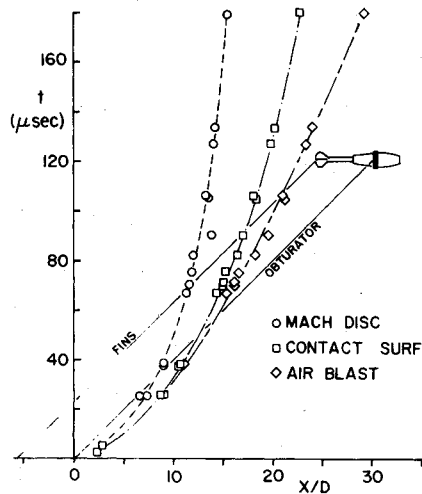


Fig. 3 Discontinuity trajectories along the axis of symmetry.

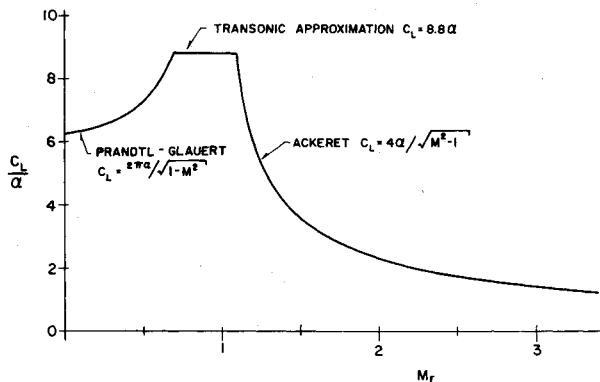


Fig. 4 Lift coefficient vs relative Mach number.

coupled jet and blast flows; however, the spark shadowgraph survey demonstrates that the fins traverse the quasisteady, supersonic core of the jet unaffected by the unsteady shock layer until relatively late times. Erdos and Del Guidice³ compute pressure levels in the shock layer to vary between 3 and 4 atm during the period of fin residence. Since the pressures near the muzzle are on the order of 600 atm, the effect of the shock layer is neglected, and the projectile is assumed to enter free flight immediately upon penetration of the Mach disk. The flow properties in the muzzle jet were computed using an axially symmetric method of characteristics code⁹ (Fig. 5).

The resulting nondimensional lift, Eq. (2), on a typical finned projectile in transit of such a flowfield is presented in Fig. 6 for various values of V_p/c_i . For values of this parameter which are less than one, the effect of the in-bore expansion is evident. The lift begins to increase at the point within the gun tube where the first expansion wave propagating back upstream from the muzzle intersects the fin.

$$X_i/D = -(d/D)[1 - (V_p/c_i)] \quad (3)$$

where d is the distance between the obturator and the fins. As the fins penetrate the expansion fan, the lift increases with relative flow velocity to a maximum at the muzzle. Since the muzzle is always the sonic point, the value of \bar{L} is only a function of V_p/c_i and is independent of d/D . For values of V_p/c_i equal to or greater than one, there is no in-bore expansion, and transverse gasdynamic loadings are generated only in the muzzle blast.

Exterior to the muzzle, \bar{L} rises initially because of continued increase in the relative flow velocity, and subsequently decays because of decreasing local flow density (Fig. 5). For

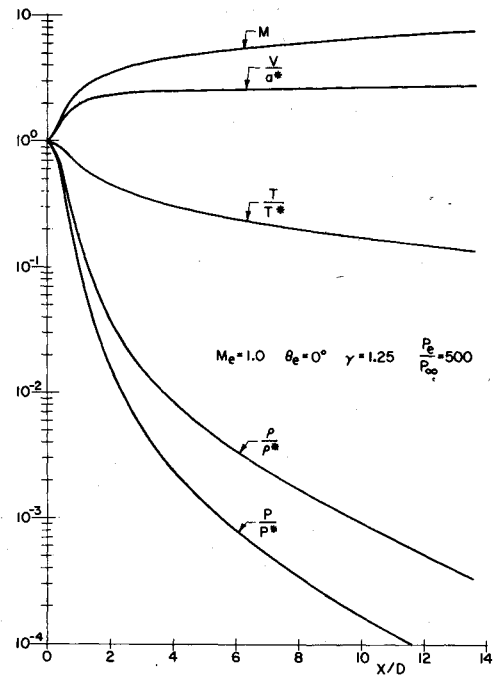


Fig. 5 Centerline property distribution in underexpanded jet.

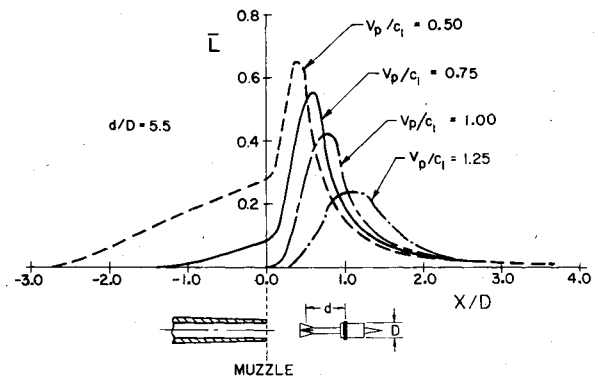


Fig. 6 Computed fin lift function.

supersonic exit conditions, $V_p/c_i > 1.0$, the relative velocity between the projectile and propellant gases remains zero until the projectile passes the two-dimensional, Prandtl-Meyer expansion from the muzzle edges; therefore, the lift function does not begin to increase until some distance downstream of the muzzle.

The lift functions presented in Fig. 6 were calculated for a single, two-dimensional airfoil traversing the prescribed flow. For a multiple-fin projectile ($n \geq 3$), Fansler and Schmidt¹⁰ show that the total lift due to the fin assembly is independent of roll angle and acts in the plane formed by the flow velocity vector and projectile axis. Additionally, they demonstrate that the loading on an n -finned assembly is equivalent to that on a two-fin assembly with its fins oriented perpendicular to the aforementioned plane and with a total fin area equal to $n/2$ times the area of a single fin.

The momentum transferred to the projectile is equal to the integral of the lift function

$$P = \frac{n}{2} \int_{t_1}^{t_2} L dt \quad (4)$$

where P is the momentum imparted to the projectile due to fin lift over the period between t_1 , when the fins first intercept the muzzle expansion, and t_2 , when the fins penetrate the Mach disk. X-ray surveys⁵ indicate that the projectile velocity and

angle of attack remain nearly constant during transit of the muzzle region; thus, Eq. (4) may be transformed to yield

$$P = \frac{D}{V_p} (\gamma + 1) p^* \frac{n}{2} A \alpha \int_{X_1}^{X_2} \bar{L} d\bar{X} \quad (5)$$

where $\bar{X} = X/D$. The integral on the right-hand side of Eq. (5) is defined as the dimensionless momentum function

$$\bar{P} = \int_{X_1}^{X_2} \bar{L} d\bar{X} \quad (6)$$

The limits of integration may be split to produce dimensionless momentum functions due to in-bore, \bar{P}_I , and external, \bar{P}_E loadings

$$\bar{P}_I = \int_{X_1}^0 \bar{L} d\bar{X} \quad (7)$$

$$\bar{P}_E = \int_0^{X_2} \bar{L} d\bar{X} \quad (8)$$

Use of Eq. (3) permits \bar{P}_I to be expressed as

$$\bar{P}_I = \frac{d}{D} \int_{X_1/d}^0 \bar{L} d(X/d) \quad (9)$$

The in-bore flow is assumed to be a centered expansion which is a similarity flow;⁸ thus, it may be shown¹⁰ that the preceding integral is independent of the fin setback distance d and varies only as a function of V_p/c_1 . Evaluation of \bar{P}_I for $d/D = 1.0$ (Fig. 7) and various V_p/c_1 permits the calculation of \bar{P}_I for any d/D by linear extrapolation, i.e.

$$\bar{P}_{I(d/D=\eta)} = \eta \bar{P}_{I(d/D=1.0)} \quad (10)$$

The value of \bar{P}_E is equal to the area under the lift curves (Fig. 6). The upper limit of integration is set at the point where the fins penetrate the Mach disk, the position of which is dependent upon muzzle exit conditions. However, the rapid decay of the lift function causes the momentum function to asymptote to a nearly constant value by $X/D = 4.0$. As a result, the effect of variations of X_2 on the value of the integral is weak, and the external momentum function is dependent only upon the propellant gas Mach number prior to shot ejection (Fig. 7).

Examination of Fig. 7 shows that as V_p/c_1 increases toward unity, the in-bore momentum function decays, since at the sonic condition no waves propagate into the gun tube and

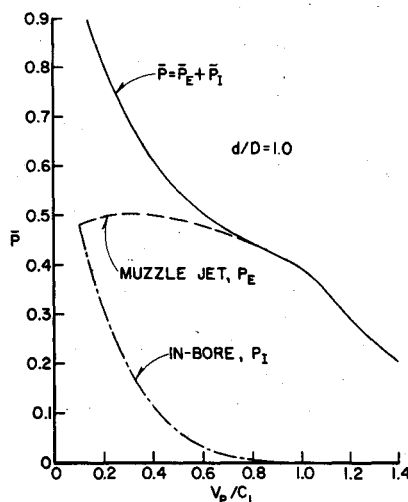


Fig. 7 Computed momentum transfer function.

reverse flow does not commence until the fins pass the muzzle. Over the same range of V_p/c_1 , the muzzle jet momentum function varies only slightly. Apparently, this is because of the counterbalancing effects of decreasing relative velocity and increasing residence in the transonic regime where the lift coefficient (Fig. 4) is a maximum. However, once the exit conditions become supersonic, \bar{P}_E decreases rapidly with increasing V_p/c_1 . When the in-bore and muzzle jet momentum functions are summed, the momentum transfer function is observed to decrease with increasing launch Mach number. Thus, according to this analysis, the influence of launch gasdynamics is more significant in low-velocity weapons such as mortars than in high-velocity weapons such as antitank rounds.

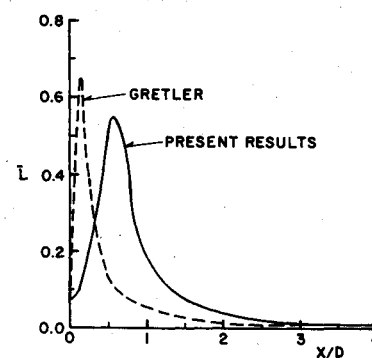
The present analysis is based upon the work of Gretler.⁴ Aside from consideration of in-bore flow, the major modification to his analysis is the incorporation of a characteristics calculation of the quasisteady core flow. Gretler makes direct use of the spherical source model of Oswatitsch.¹ The more rapid flow expansion predicted by the source model is reflected in the resulting lift and momentum functions (Fig. 8). The lift function computed by Gretler reaches a maximum and decays significantly sooner than the present model. Since the momentum function is the area under the lift curve, the momentum function predicted by Gretler is approximately one-half that obtained with the present approach. These plots demonstrate the importance of accurately depicting the flow near the muzzle where maximum loadings occur.

Projectile Deflection

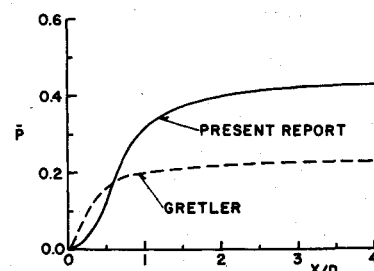
The assumption that the projectile traverses the muzzle flow region at a constant velocity V_p and angle of attack α permits a straightforward integration of the equations of motion which yields the following closed-form expressions for transverse linear and angular velocities upon entry into flight.

$$w/V_p = (\gamma + 1) p^* (n/2) A \alpha (D/m_p V_p^2) \bar{P} \quad (11)$$

$$\alpha' = (\gamma + 1) p^* (n/2) A \alpha (\Delta D/I, V_p^2) \bar{P} \quad (12)$$



a) Lift function



b) Momentum transfer function

Fig. 8 Comparison of the present results with those of Gretler.⁴

Table 1 Muzzle blast induced dispersion

	5.8-mm flechette	60-mm mortar	90-mm APDS
V_p , m/sec	1460	120	1480
Measured distribution in α	0.16°	0.20°	0.10°
Total measured dispersion, mils	1.30	2.50	0.30
Calculated muzzle blast dispersion, mils	0.012	0.40	0.02

The transverse linear velocity results directly in a deflection of the projectile from its intended trajectory; however, the effect of angular velocity is more complicated, requiring knowledge of projectile aerodynamics and subsequent oscillatory motion. The equations of motion of a statically stable missile have been integrated by Murphy and Bradley.¹¹ They obtain the following expression for the aerodynamic jump, i.e., the deflection of the trajectory due to projectile yawing motion.

$$\theta_j = (I_y/m_p l^2) (C_{L_\alpha}/C_{M_\alpha}) \alpha' \quad (13)$$

Substitution of Eq. (12) into Eq. (13) yields

$$\theta_j = (C_{L_\alpha}/C_{M_\alpha}) (\gamma + 1) p^* (n/2) A \alpha (\Delta D/m_p V_p^2 l) \bar{P} \quad (14)$$

The total deflection of the projectile trajectory is the vector sum of the transverse linear velocity, Eq. (11), and the aerodynamic jump, Eq. (14)

$$\theta = [1 + (C_{L_\alpha}/C_{M_\alpha}) (\Delta/l)] (\gamma + 1) p^* (n/2) A \alpha (D/m_p V_p^2) \bar{P} \quad (15)$$

Because of the simplifying assumptions in the analysis, this expression produces an upper bound on the effect of transverse muzzle gasdynamic loadings upon deviation of the round from the intended line of fire. The expression is a function of the projectile's inertial, aerodynamic, and launch properties. If statistical variations in these properties from round to round were known, it would be possible to use Eq. (15) to estimate the contribution of muzzle blast loadings to dispersion. Of the parameters in Eq. (15), variation in launch angle of attack is anticipated to have the greatest impact upon muzzle blast induced dispersion. The magnitude of this dispersion was calculated for a variety of fin-stabilized projectiles and is summarized in Table 1.

Based on the (one-sigma) standard deviation in projectile angle of attack at the muzzle, the resultant dispersion about the aim point due to muzzle dynamic loadings is shown in the fourth row. For the two high-velocity launch cases, the contribution of muzzle blast to the total measured dispersion is negligible. The mortar calculation shows that the muzzle blast is a more significant, although by no means dominant, source of dispersion. Since the present model is an overestimate, it must be concluded that muzzle gasdynamic loadings are not a significant source of dispersion.

Model Validation

Direct measurement of loadings transmitted to projectiles in transit of the muzzle region is not possible; therefore, observations of the downrange dynamics of a projectile are used to infer the properties of the launch environment. In general, downrange motion caused by muzzle gasdynamic loadings may not be separated from that due to mechanical loadings. To provide such separation, it is necessary to introduce artificial constraints. This approach is taken here. An adaptor (Fig. 9) is installed on the muzzle of the 5.8-mm, smoothbore gun previously tested. The adaptor is designed to enhance gasdynamic loadings while leaving mechanical loads unaltered. As may be seen from Fig. 9, the device is a nozzle which prohibits free expansion of the propellant gases; rather,

they are directed to form a high-velocity, high-density stream over the projectile.

In launching the 1.13-g flechette at a velocity V_p of 1473 m/sec, the following propellant gas properties at shot ejection are calculated.¹²

$$\gamma_I = 1.25$$

$$R = 399.2 \text{ m}^2/\text{sec}^2 \text{K}$$

$$M_I = V_p/c_I = 1.68$$

$$p_I = 428.6 p_\infty$$

The expansion of the propellant gas into the adaptor, $A/A_I = 4.0$, is calculated assuming steady, quasi-one-dimensional flow; thus

$$M = 2.95$$

$$p = 48.9 p_\infty$$

$$M_r = 0.86$$

A projectile travelling through this adaptor at angle of attack will experience significant transverse gasdynamic loading over a longer portion of its initial flight path than is the case with a bare muzzle (25 calibers compared against two calibers, Fig. 6). The impact of these loadings on the trajectory of the round may be computed in a manner analogous to that presented in the previous sections. For the relative Mach number in the adaptor, $C_{L_\alpha} = 8.8$. A lift force is defined by Eqs. (1) and (2). Because of the length of the muzzle adaptor, the projectile angle of attack no longer may be assumed constant; however, the equations of motion are a simple set of second-order ordinary differential equations with constant coefficients. The solution of these equations is straightforward,¹³ and the expression for the trajectory deflection due to the gas loadings in the adaptor is

$$\theta = -0.114\alpha - 4.52\alpha' \quad (16)$$

The round-to-round distributions in the values of both α and α' just as the flechette separates from the gun tube have been measured using x-ray techniques⁵ (Figs. 2b and c). These data were taken in firings from the gun without the muzzle adaptor present. If this initial distribution due to in-bore mechanical interactions is assumed to be unchanged by the addition of the muzzle adaptor, the increase in dispersion predicted by the present theory can be calculated by substituting the measured launch yaw properties into Eq. (16). A comparison between measured and predicted dispersion is presented in Fig. 10.

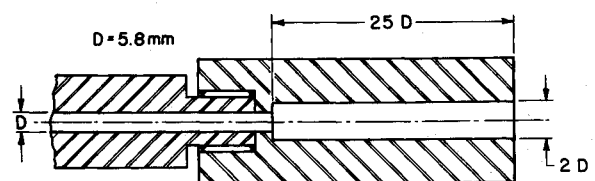


Fig. 9 Gasdynamic amplifier.

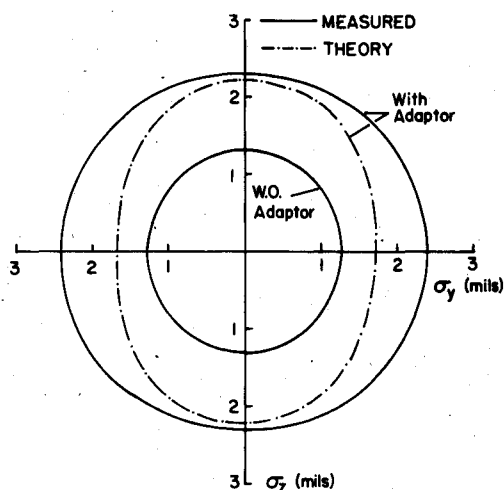


Fig. 10 Comparison of measured and predicted dispersion patterns.

Two groups of ten rounds each were fired – one group with the muzzle adaptor mounted and the second without it. The variation in projectile trajectory was measured by recording impacts into a target placed 30-m downrange. The dispersion patterns shown in Fig. 10 represent one-standard-deviation boundaries about the mean point of impact (i.e., 68% of the impacts occur within these contours). The addition of the muzzle adaptor causes a 1-mrad growth in the size of the measured dispersion pattern. Although the measured impact patterns are both roughly circular, the theory predicts an elliptical distribution. This reflects the statistical nature of the input data. The elliptical distribution is a direct result of the distribution in α and α' , obtained from measurements of eight separate firings. Thus, considering the relatively small number of rounds fired to generate both the impact patterns (10) and input data (8), the agreement between measurement and theory is quite good. This is taken as a confirmation of the validity of the general approach to the analysis of muzzle blast loadings upon fin-stabilized projectiles.

Summary and Conclusions

Optical and x-ray photographs are presented which define the muzzle blast flowfield about weapons firing fin-stabilized projectiles. Based on these experimental results, an analysis is developed permitting the computation of the magnitude of gasdynamic loadings of fin-stabilized projectiles during launch. Both in-bore loadings due to the unsteady expansion propagating upstream and external loadings generated in transit of the muzzle blast are considered. The in-bore flow is modeled as a one-dimensional, unsteady expansion fan; whereas the external flow is approximated as a quasisteady underexpanded jet. The transverse loadings on the projectile are assumed to be generated dominantly on fin surfaces. As such, they are calculated using two-dimensional thin airfoil theory.

The analysis of the in-bore flow is highly idealized; however, it provides an estimate of the magnitude, duration, and relative importance of loadings seen by the projectile in

this region. The momentum transferred to the projectile is shown to be a function of propellant gas properties prior to separation of the obturator and the standoff distance between the obturator and the fins. For high-velocity guns, in-bore loadings may be neglected; however, for low-velocity guns, such as mortars, they must be considered. The method-of-characteristics calculation of the external flow used in this report is shown to produce momentum impulses significantly greater than those previously computed using source flow models.

The assumptions made to simplify the analysis result in a solution which is generally applicable to any projectile fin configuration provided that the sabot design is a center or forward puller. Weapon characteristics enter the solution in a straightforward manner, permitting direct computation for any caliber, launch velocity, or exit pressure. Additionally, the assumptions produce an upper bound on the magnitude of muzzle blast loadings. This permits the simplistic approach contained in this report to be used to estimate projectile dispersion due to muzzle blast loads. From the calculation of this dispersion for three different weapons, it is concluded that muzzle gasdynamic loadings are not a significant source of dispersion.

References

- ¹Oswatitsch, K., "Intermediate Ballistics," Deutschen Versuchsanstalt für Luft- und Raumfahrt, Aachen, Germany, DVL R 358, June 1968.
- ²Schmidt, E. M. and Shear, D. D., "Optical Measurements of Muzzle Blast," *AIAA Journal*, Vol. 13, Aug. 1975, pp. 1086-1091.
- ³Erdos, J. I. and Del Guidice, P., "Calculation of Muzzle Blast Flowfields," *AIAA Journal*, Vol. 13, Aug. 1975, pp. 1048-1055.
- ⁴Gretler, W., "Intermediate Ballistics Investigations of Wing Stabilized Projectiles," Deutschen Versuchsanstalt für Luft- und Raumfahrt, Aachen, Germany, R 67-92, Nov. 1967.
- ⁵Schmidt, E. M. and Shear, D. D., "Launch Dynamics of a Single Flechette Round," Ballistic Research Laboratory, Aberdeen Proving Ground, Md., R 1810, Aug. 1975.
- ⁶Glauz, W. D., "Estimation of Forces on a Flechette Resulting from a Shock Wave," Midwest Research Institute, Kansas City, Mo., Final Rept. Project 3451-E, May 1971.
- ⁷Schmidt, E. M., Gion, E. J., and Shear, D. D., "Acoustic Thermometric Measurements of Propellant Gas Temperatures in Guns," *AIAA Journal*, Vol. 15, Feb. 1977, pp. 222-226.
- ⁸Landau, L. D. and Lifshitz, E. M., *Fluid Mechanics*, 1st ed., Pergamon, London, 1959, pp. 353-360.
- ⁹Vick, A. R., Andrews, E. H., Dennard, J. S., and Craiden, C. B., "Comparison of Experimental Free-Jet Boundaries with Theoretical Results Obtained with the Method of Characteristics," NASA TN D-2327, June 1964.
- ¹⁰Fansler, K. S. and Schmidt, E. M., "The Influence of Muzzle Gasdynamics upon the Trajectory of Fin-Stabilized Projectiles," Ballistic Research Laboratory, Aberdeen Proving Ground, Md., R 1793, June 1975.
- ¹¹Murphy, C. H., "Free Flight Motion of Symmetric Missiles," Ballistic Research Laboratory, Aberdeen Proving Ground, Md., R 1216, July 1963.
- ¹²Baer, P. G. and Frankle, J. M., "The Simulation of Interior Ballistic Performance of Guns by Digital Computer Program," Ballistic Research Laboratory, Aberdeen Proving Ground, Md., R 1183, Dec. 1962.
- ¹³Schmidt, E. M., "Muzzle Blast Amplification," Ballistic Research Laboratory, Aberdeen Proving Ground, Md., R 1945, Nov. 1976.